
OBSERVATION OF ALFVÉN WAVE IN ICME-HSS INTERACTION REGION

A PREPRINT

Omkar Dhamane^{1*}, Anil Raghav¹, Zubair Shaikh², Utsav Panchal¹, Kalpesh Ghag¹, Prathmesh Tari¹,
Komal Chorghé¹, Ankush Bhaskar³, Wageesh Mishra⁴

¹Department of Physics, University of Mumbai, Mumbai, India

²Indian Institute of geomagnetism, Panvel, Navi Mumbai, India

³Vikram Sarabhai Space Centre (VSSC), Indian Space Research Organisation (ISRO), Thiruvananthapuram, Kerala 695022, India

⁴Indian Institute of Astrophysics, II Block, Koramangala, Bengaluru 560034, INDIA *anil.raghav@physics.mu.ac.in

September 13, 2022

ABSTRACT

The Alfvén wave (AW) is the most common fluctuation present within the emitted solar wind from the Sun. Moreover, the interaction between interplanetary coronal mass ejection (ICME) and high-speed stream (HSS) has been observed on several occasions. However, can such interaction generate an AW? What will be the nature of AW in such a scenario remains an open question. To answer it, we have investigated an ICME-HSS interaction event observed on 21st October 1999 at 1 AU by Wind spacecraft. We have used the Walén test to identify AW and estimated Elsaesser variables to find the characteristics of the AWs. We explicitly find that ICME were dominant with Sunward AWs, whereas the trailing HSS has strong anti-Sunward AW. We suggest that the ICME-HSS interaction deforms the MC of the ICME, resulting in the AWs inside the MC. In addition, the existence of reconnection within the ICME early stage can also be the leading cause of the origin of AW within it.

Keywords

Coronal mass ejection (CME) – High speed stream(HSS) – Alfvén wave

1 Introduction

Coronal mass ejection (CME) is a massive expulsion of considerable volumes of plasma with immense energy flows outward at speeds ranging from 10 to around 2,000 km s⁻¹ from the solar corona (Hundhausen, 1999). CMEs are the primary source of space weather disruptions in the heliosphere and planetary environments. Their relative excess speed over the ambient solar wind speed forms the shock front and sheath region (Kilpua et al., 2017a). Thus, it was proposed that the CME possesses a bubble or loop-like structure well behind the shock (Hirshberg et al., 1970; Gosling et al., 1973; Palmer et al., 1978). When a CME moves from the near-Sun region to the interplanetary medium, its kinematic configuration evolves. During the solar maximum, more CMEs are ejected from the sun, resulting in their frequent collisions that lead to the deformation of the structure. ICMEs are the Interplanetary counterparts of CMEs observed in the heliosphere using in-situ data. ICMEs causes extreme geomagnetic storms (Zurbuchen & Richardson, 2006; Zhao & Dryer, 2014; Kilpua et al., 2017b). Their strong and hazardous impacts on Earth's space weather are difficult for current spacecraft technology to handle (Board et al., 2009). The ICME research has received a lot of interest due to its importance in both scientific and technical implications (Webb & Howard, 2012; Schrijver & Siscoe, 2010; Cannon et al., 2013).

The ICME propagates in the sea of solar wind. The solar wind is an effect of the supersonic expansion of the solar corona (Gosling & Pizzo, 1999). Generally, it is distinguished into two classes: fast solar wind (speed > 500 km/s) and slow solar wind (speed < 500 km/s). The Speed is not only a parameter to differentiate, but their relative composition also characterizes the steady bulk plasma properties (Axford & McKenzie, 1992). The fast solar wind has its origin

in coronal holes (CHs) in the Sun, especially in the solar polar region (Vršnak et al., 2007; Gosling & Pizzo, 1999). Moreover, the periods of fast solar wind that continue more than one day are referred to as high-speed solar wind streams (HSS) (Denton et al., 2008; Xystouris et al., 2014; Mavromichalaki & Vassilaki, 1998). HSS can result from a single or several CHs (Gupta et al., 2010; Kumar et al., 2014). The kinetic energy is transformed to thermal energy in the fast solar wind zone, resulting in plasma heating and expansion (Alves et al., 2006). When ICME travels in heliosphere via solar wind, its interaction particularly with HSSs can significantly affect ICME properties thus faces several types of deformation such as; the embedded flux rope may bend, kink, rotate, or become distorted (Riley & Crooker, 2004; Wang et al., 2006; Manchester IV et al., 2004). Moreover, the interaction between ICME-HSS may result in reconnection between them.

There are ample of observations of micro-scale plasma and magnetic fluctuations that indicates generation of plasma waves in the macro-scale structure of the interplanetary medium. Researchers have focused on both theoretical and empirical investigations of such waves due to their importance in dynamical processes inside the solar wind as well as their effect on geophysical phenomena. In fact, plasma turbulence can take the form of Alfvén waves, Whistler waves, ion cyclotron waves, or ion Bernstein waves (Krishan & Mahajan, 2004; Salem et al., 2012; Shaikh, 2010; Gary & Smith, 2009). Gamayunov et al. (2018) investigates the statistics of electromagnetic ion cyclotron (EMIC) waves detected in the Earth’s inner magnetosphere during ICMEs, HSS, and quiet solar wind conditions in the upstream solar wind. Several observational investigations imply that small variations in the solar wind, particularly ultralow frequency (ULF) waves, can affect magnetospheric dynamics, particularly during HSS (McGregor et al., 2014). Kanekal et al. (2015) demonstrated an uncommon interplanetary driver combination, with a CME embedded in an HSS, resulting in a complicated response of the outer zone radiation belt electrons. There was increased ULF and chorus wave activity shortly prior to, and extending throughout, the energization period during both HSS and shock/sheath passage. Miyoshi et al. (2013) studied long-term plasma data sets and showed that relativistic electrons in outer radiation belt are accelerated by whistler mode waves during HSS events.

Several studies have proven the importance of Alfvén waves or Alfvénic turbulence in geomagnetic storm dynamics (e.g., Tsurutani & Ho (1999); Telloni et al. (2021) and references therein). Tsurutani & Gonzalez (1987) claimed that Alfvénic fluctuation in fast solar streams is linked to a prolonged recovery profile in high-intensity long-duration continuous AE activity (HILD- CAAs) events. Similarly, the extended recovery profiles of ICME-induced geomagnetic storms are attributed to Alfvénic fluctuations inside the ICME substructures. (Raghav et al., 2018, 2019; Shaikh et al., 2019b). Furthermore, Shaikh et al. (2019b) revealed that Alfvénic fluctuations not only slow down the storm’s recovery profile. Recently, it was shown that during the storm’s main phase, the hemisphere Alfvénic power surged by four times when compared to non-storm periods (Keiling et al., 2019). Thomas & Pfrommer (2019) postulated that cosmic ray energy and Alfvén waves may be exchanged via the gyroresonant instability. They further show that cosmic ray interactions with Alfvénic turbulence are the primary driver of cosmic ray scattering. Chaston et al. (2007) hypothesized that auroral particles can be accelerated by Alfvén waves. Moreover, Bellan & Stasiewicz (1998) suggested that Alfvén Wave Ponderomotive Force creates cavity into the Ionospheric Plasma. Even Chaston et al. (2006) hypothesized that Alfvén waves cause ionosphere erosion. Recently, Hull et al. (2019) suggest that the dispersive Alfvén waves have recently become quite essential in the energization of O^+ ions in the inner magnetosphere. Alfvén wave also plays significant role in plasma heating (Hasegawa & Chen, 1974), transportation (e.g., Chen & Zonca (2016); Hasegawa & Chen (1975) and references therein), magnetotail dynamics (Keiling, 2009), auroral dynamics (Stasiewicz et al., 2000), etc. Therefore, it is important to investigate the origin and propagation of the Alfvén wave and related processes in space plasma.

The structural configuration of large scale magnetic structures is altered by interactions such as CME-CME, CME-HSS, CME-CIR etc. Heinemann et al. (2019) showed the signature of Stream interface(SI) as the HSS passes the slow solar wind resulting in drop of proton density and sharp increase in temperature. They further pointed out that the HSS is followed by CME and their interaction gives sharp rise in magnetic field, proton density, velocity and temperature corresponding to shock sheath region. Theoretical studies also suggest that when large-scale magnetic structures interact, momentum and energy are transferred in the form of an MHD wave Jacques (1977). Raghav et al. (2018) investigated a CME-CME interaction event, discovered torsional Alfvén waves in the MC region. Moreover, Alfvénic fluctuations were found at the stream interface of fast and slow solar wind interaction (Lepping et al., 1997; Tsurutani et al., 1995). Here, we present first observation of Alfvén waves generation caused by interaction between CME and following HSS.

2 Data, Methods & Observations

We examined, ICME-HSS interaction event that observed by the Wind spacecraft on 21st October 1999. We used 92-second temporal resolution data of the plasma and magnetic field in GSE coordinates to examine the interplanetary conditions during the passage of interaction region. Moreover, to determine the presence of Alfvén waves, we analysed

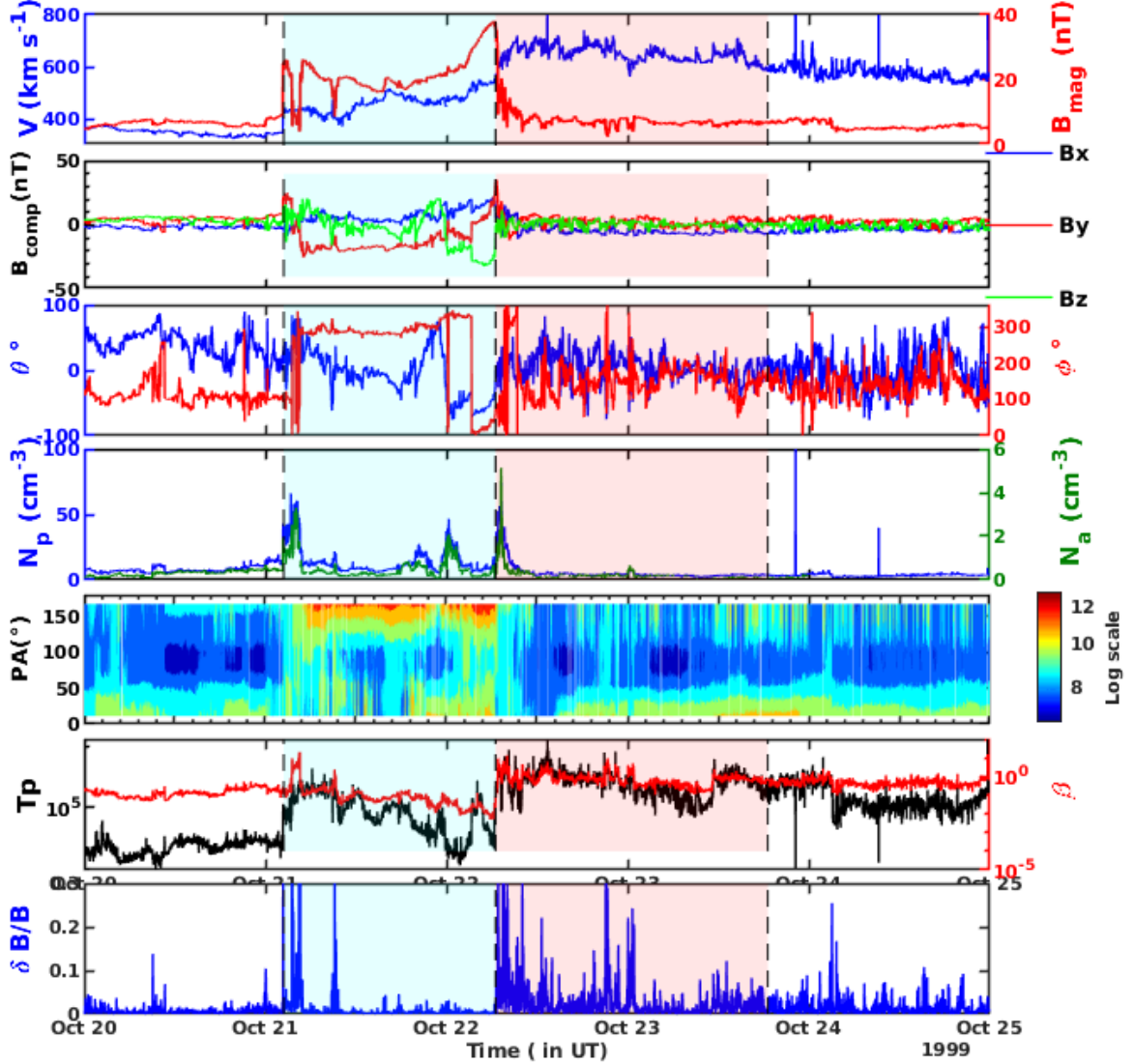


Figure 1: Wind observation of complex ICME–HSS interaction event on 1999 October 20–24 (time cadence of 92 s). Total interplanetary field strength IMF B_{mag} in nT and total solar wind V (km s^{-1}) are shown in the top panel. Components of the magnetic field are shown in the second panel. Third panel displays the IMF orientation (θ, ϕ). In the fourth panel, the proton number density (N_p) is represented on the left, while α is shown on the right. The pitch angle (PA) of superthermal electron strahls is depicted in the fifth panel. The proton temperature (T_p) and the β value were plotted in the sixth panel on the left side and the right side, respectively. The plot of $\delta B/B$ is demonstrated in the last panel.

high resolution data from onboard wind satellite sensors such as wind MFI and 3DP with a 3-sec resolution. The data is available at <https://wind.nasa.gov/data.php>.

2.1 Interplanetary conditions

The interplanetary conditions during the passage of ICME-HSS interaction region is demonstrated in Figure 1. A sudden sharp enhancement is observed in total interplanetary magnetic field (IMF), plasma density, and solar wind speed suggesting the onset of ICME at 02:19 hr on 21 October 1999. The low plasma beta (β) and low fluctuations in IMF indicate the magnetic cloud (MC) crossover. The electron pitch angle shows nearly bidirectional flow that confirms a possible closed magnetic structure. The rear-end is observed at 06:29 hr on 22 October 1999. The ICME boundaries are also confirmed by ICME catalogue available at https://wind.nasa.gov/ICME_catalog/ICME_catalog_viewer.php

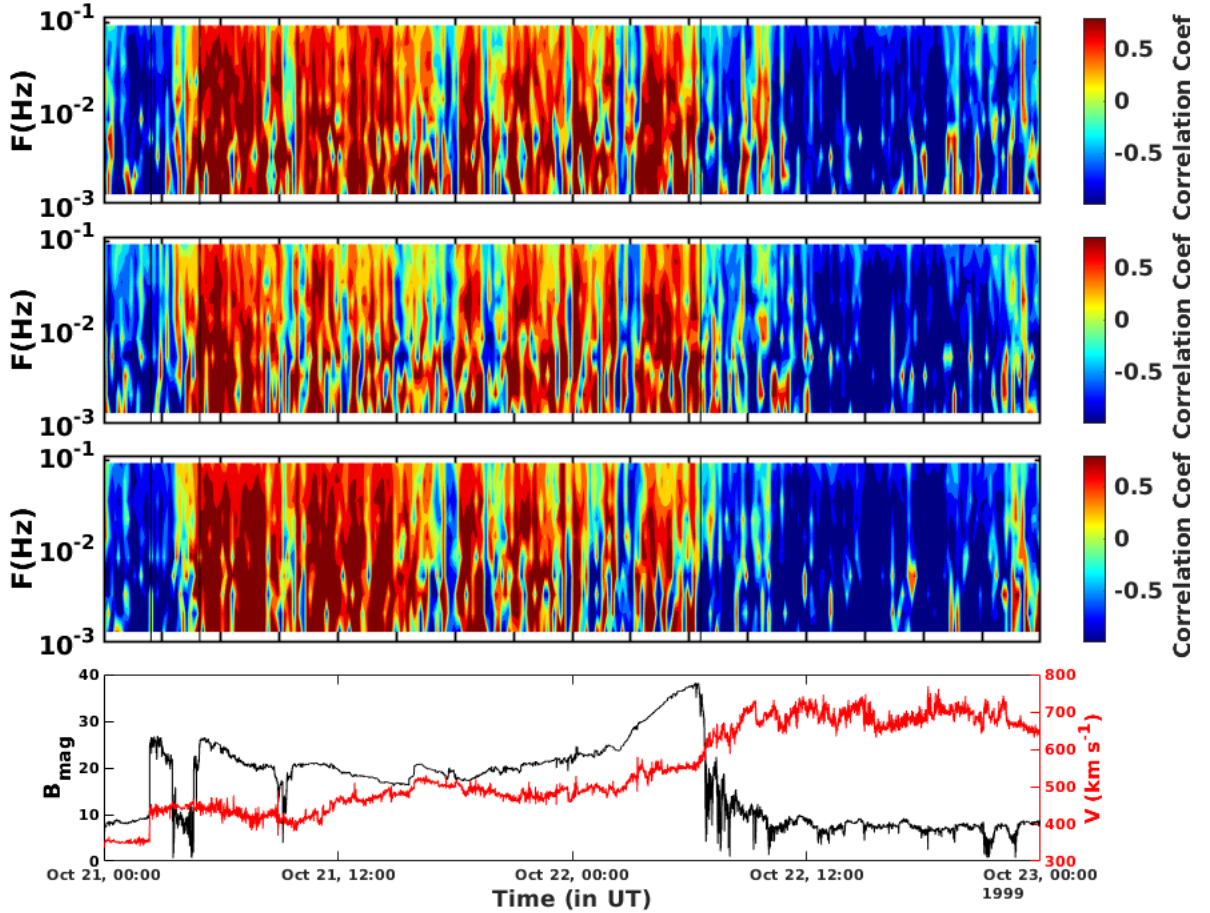


Figure 2: In the time frequency domain, the correlation coefficient between V_{Ai} and V_I for a ICME-HSS event are presented. The bottom shows total magnetic field(B_{mag}) and solar wind velocity (V) is plotted for reference.

In general, the MC of ICMEs depicts gradual decrease in total IMF and solar wind speed that implies the expansion of MC in solar wind. However, in studied event, the trailing edge of MC demonstrates anomalous behaviour such as; rise in total IMF and solar wind speed. Thus, It is clearly visible that observed ICME MC completely contradicted to conventional definition of MC. The anomalous behaviour at the trailing edge of ICME MC could be due the existence of HSS flow from behind which is evident as high speed stream. The compression of ICME MC by the HSS causes the plasma particles to pile up at the trailing end along with the high IMF fluctuations (Rodriguez et al., 2016). Thus we thought that the MC is distorted due to the ICME-HSS interaction and HSS may cause turbulence at the rearer end of MC. As a result of this deformation, the force balance conditions of the ICME flux rope may altered. In addition to this, at the leading part of the ICME we observe two sharp dips in the total magnetic field, which coincides with rise in proton and alpha density and plasma temperature. It can be interpreted as magnetic reconnection exhaust based on reported literature(Gosling et al., 2005).

2.2 Alfvén wave identification

Alfvén waves are the most basic form of fluctuation in a magnetic plasma commonly identified in the solar wind across the heliosphere (Alfvén, 1942; Belcher & Davis Jr, 1971). The velocity of Alfvén fluctuations is defined as,

$$\Delta V_A = \frac{\Delta B}{\sqrt{\mu_0 \rho}} \quad (1)$$

here, $\Delta B = B - B_{avg}$ is the fluctuations in the respective components of IMF. Correct assessments of their fluctuations are based on accurate estimation of background values. In literature, a precise de Hoffmann-Teller frame or mean values are utilized as a background value to diagnose the existence of interplanetary Alfvén waves (Raghav & Kule, 2018; Raghav et al., 2018; Yang & Chao, 2013; Gosling et al., 2009). However, in HSS, the HT frame might vary rapidly (Gosling et al., 2009; Li et al., 2016), and the use of average value as the background state isn't always appropriate. As a result, during the examined CME-HSS interaction, we employed another technique to identify large-amplitude Alfvén waves. The whole data set under analysis is divided into ten-minute time intervals. Each time window's data was then passed through the 4th order Butterworth filter (via the MATLAB software). We choose 10 periodic bands for bandpass filter as 10s-15s, 15s-25s, 25s-40s, 40s-60s, 60s-100s, 100s-160s, 160s-250s, 250s-400s, 400s-630s, and 630s-1000s in an evenly distributed manner. In our study, the Alfvénic waves are observed in frequency bands between 10^{-3} to 10^{-1} Hz. Finally, the Walén relation is used to determine the relationship between the components of Alfvén and the solar wind velocity as,

$$\Delta V_i = |R_{Wi}| \Delta V_{Ai} \quad (2)$$

where R_w is known as Walén slope which represent the linear relationship between ΔV_A and ΔV . Furthermore, the presence of Alfvén waves or Alfvénic fluctuations in the examined region was demonstrated by the correlation coefficient (CC) between respective components of V_i and V_{Ai} . The Figure 2 demonstrates the existence of Alfvén waves during interval of ICME-HSS interaction. The colour-bar shows Pearson correlation coefficient (CC) between components of ΔV_A and ΔV . For CC = -1 (dark blue shade) implies existence of anti-Sunward Alfvén waves, whereas, CC = 1 (dark red shade) means Sunward Alfvén waves. Top three panels shows frequency dependent distribution of CC between the respective components (x, y, & z) of ΔV_A and ΔV . A negative CC observed at the ICME upstream solar wind and trailing HSS region. In contrast, during the ICME transit mostly we observed positive CC. It implies that the ICME is superimposed with dominant Sunward Alfvén waves, whereas the trailing HSS show strong anti-Sunward flow.

2.3 Characteristics of Alfvén wave

Generally, Elsässer variables are used to characterize the solar wind turbulence and Alfvén wave properties (Elsasser, 1950; Marsch & Mangeney, 1987; Bruno & Carbone, 2013a). Here, we employed them to distinguish the dominant flow of outward and inward Alfvénic fluctuation (Elsasser, 1950; Marsch & Mangeney, 1987; Bruno & Carbone, 2013a). The Elsässer variables are define as;

$$\vec{z}^{\pm} = \vec{V} \pm \frac{\vec{B}}{\sqrt{4\pi\rho}}, \quad (3)$$

here, \vec{V} and \vec{B} are fluctuations in proton velocity and magnetic field respectively. The \pm sign in front of \vec{B} depends on the sign of $[-k \cdot B_0]$. If both velocity and magnetic field are directed outward The above equation 3 modified as $z^{\vec{+}} = \vec{V} - \vec{V}_A$ and $z^{\vec{-}} = \vec{V} + \vec{V}_A$. On the other hand, magnetic field points in the direction of the sun, the correlation sign is reversed (v always outward), and $z^{\vec{+}} = \vec{V} + \vec{V}_A$ and $z^{\vec{-}} = \vec{V} - \vec{V}_A$ are the results. In this sense, z^+ & z^- represents an outward & inward Alfvénic mode respectively, at all times. (Roberts et al., 1987; D'Amicis & Bruno, 2015; Bruno & Bavassano, 1991) The Figure 3 represents the characteristic of Alfvén wave for the studied region of interest. The top three panels clearly shows that components of ΔV and ΔV_A are either correlated or anti-correlated with each other. It implies that the existence of Alfvén wave in the studied region exhibits both outward and inward propagation nature. To have better clarity in the time evolution of outward and inward propagation of wave, we have demonstrated ratio of z^-/z^+ , normalized cross helicity (σ_c), angle between $\vec{\Delta V}$ and $\vec{\Delta V}_A$ (θ), normalized residual energy (σ_R) in the Figure 3.

We found mean value of ratio of Elsässer variables as ~ 0.54 in HSS region whereas ~ 2.13 inside the ICME MC. In fact, the temporal fluctuation in the ratio reached ~ 10 in the front part of MC and highly varies in the trailing part of the MC.

The normalized cross helicity (σ_c) is defined as,

$$\sigma_c = \frac{e^+ - e^-}{e^+ + e^-} \quad (4)$$

where $e^{\pm} = \frac{1}{2} (z^{\pm})^2$, e^- & e^+ are the energies related to z^- and z^+ . The normalized cross helicity shows degree of Alfvénicity (Tu et al., 1989). Moreover, $\sigma_c \sim 1$ denotes a prominent outward propagating flow whereas $\sigma_c \sim -1$ depicts a dominating inward propagating flow (Matthaeus & Goldstein, 1982; Tu et al., 1989). The analysis yielded a positive average value for HSS region i.e $\sigma_c = 0.57$, indicating predominately outward flow. Furthermore, we observed $\sigma_c = -1$ with high fluctuations in the front part of MC. Moreover, the mean value for ICME MC is found as $\sigma_c = -0.22$, implying inward flow in MC region.

To quantify the wave propagation flow direction we have also estimate angle between V and B_{mag} as follows:

$$\theta_{VB} = \cos^{-1}\left(\frac{-B_x}{B_{mag}}\right) \quad (5)$$

We frequently observed the value of θ below 30° and mean value is about 40.21° in the HSS region. It imply that the two vectors are nearly parallel in HSS region. This supports the strong outward Alfvénic flow. However, in the MC region, we observed highly fluctuating angles which sometimes reached 150° value. The mean value of the angle is observed as 109.67° .

The normalized residual energy is defined as

$$\sigma_R = \frac{e^v - e^b}{e^v + e^b} \quad (6)$$

where e^v & e^b is kinetic and magnetic energy respectively. σ_R is measure of the excess magnetic field energy with respect to kinetic energy or vice versa (Bruno & Carbone, 2013a). Analysis revealed that the value of σ_R is routinely found below one in the HSS region, whereas it is highly fluctuating in the MC region, possibly due to the mixing of inward and outward waves.

Discussion and conclusion

Alfvénic fluctuations are transverse magnetohydrodynamic (MHD) fluctuations in which ions and magnetic fields oscillate at low frequencies (Cross, 1988; Cramer, 2001). It propagates in the direction of the magnetic field, with ion mass density providing inertia and magnetic field lines providing restoring force. Alfvénic fluctuations are ubiquitous in space plasma such as; ionosphere, magnetotail (Keiling, 2009), magnetosheath, interplanetary space (Wang et al., 2012), slow solar wind (D'Amicis et al., 2019), Fast solar wind (Hollweg, 1975; Tsurutani et al., 2018), co-rotating interaction region (CIR) (Tsubouchi, 2009; Shi et al., 2020), interplanetary coronal mass ejection (ICME) sheath (Shaikh et al., 2019a) and magnetic cloud (Raghav et al., 2018), planetary region and there moon (Hinton et al., 2019), inner-heliosphere (Bavassano & Bruno, 1989a; Perrone et al., 2020), outer-heliosphere, astrophysical plasma, solar corona (Tomczyk et al., 2007; Cally, 2017), solar surface or atmosphere (Jess et al., 2009; Mathioudakis et al., 2013), lab-plasma (Gekelman, 1999, 2003), etc. The Alfvén wave shows some peculiar characteristics such as period doubling phenomena, arc polarization, and phase steepening (Riley et al., 1996a; Tsurutani et al., 2018). The origin of the Alfvén wave are associated with several physical process such as; (i) magnetic reconnection exhausts (Belcher & Davis Jr, 1971; Gosling et al., 2009), (ii) backstreaming ions from reverse shocks (Gosling et al., 2011), (iii) steepening of a magnetosonic wave, (iv) velocity shear instabilities (Bavassano et al., 1978; Roberts et al., 1992; Hollweg & Kaghshvili, 2011), (v) oblique fire-hose instability (Matteini et al., 2007; Hellinger & Trávníček, 2008), (vi) kinetic instabilities associated with proton heat flux (Goldstein et al., 2000; Matteini et al., 2013), (vii) interaction of multiple CMEs (Raghav & Kule, 2018), etc.

It is worth noting that the outward Alfvén waves are widespread in the solar wind, whereas inward Alfvén waves are uncommon (Belcher et al., 1969; Daily, 1973; Burlaga & Turner, 1976; Riley et al., 1996b; Yang et al., 2016). With growing heliocentric distance, inward Alfvén waves are expected, and they're also associated to unusual occurrences like magnetic re-connection exhausts and/or back-streaming ions from reverse shocks (Belcher & Davis Jr, 1971; Roberts et al., 1987; Bavassano & Bruno, 1989a; Gosling et al., 2009, 2011). Localised superposition of inward and outward Alfvén waves may be caused due to solar wind velocity shears effect triggered by plasma instabilities (Bavassano & Bruno, 1989b). When both Alfvén waves are present at the same time, nonlinear interactions occur (Dobrowolny et al., 1980), which is important for the dynamical evolution of a Kolmogorov-like MHD spectrum (Bruno & Carbone, 2013a). In general the solar wind is uniform and persistent in high-latitude therefore decrease in cross helicity could be induced by parametric instability (Malara et al., 2001). The helicity decrease as the heliocentric distance increases (Matthaeus et al., 2004; Bavassano et al., 2000).

Here, we demonstrated the existence of Alfvén wave during the ICME-HSS interaction at 1 AU. The observations in Figure 1 indicates that the HSS interacts with ICME from the trailing edge. As a result, the ICME MC does not appear to be expanding as expected; rather, the rise in IMF total near the rear end implies MC compression. In the B_y , B_z , and θ variations, the distortion is clearly visible (Kilpua et al., 2012). This interacting ICME-HSS event causes geomagnetic storm for longer period of time (Singh et al., 2009; Kilpua et al., 2012). Based on the observations and estimations shown in Figure 2 & 3, we gave an explicit observation of Alfvén wave during this interaction. The correlation values and temporal fluctuations in various estimated quantities from Elsässer variables, we infer that the initial part of ICME magnetic cloud superposed with a strong inward Alfvén wave flow, whereas the HSS region displayed a strong outward flow.

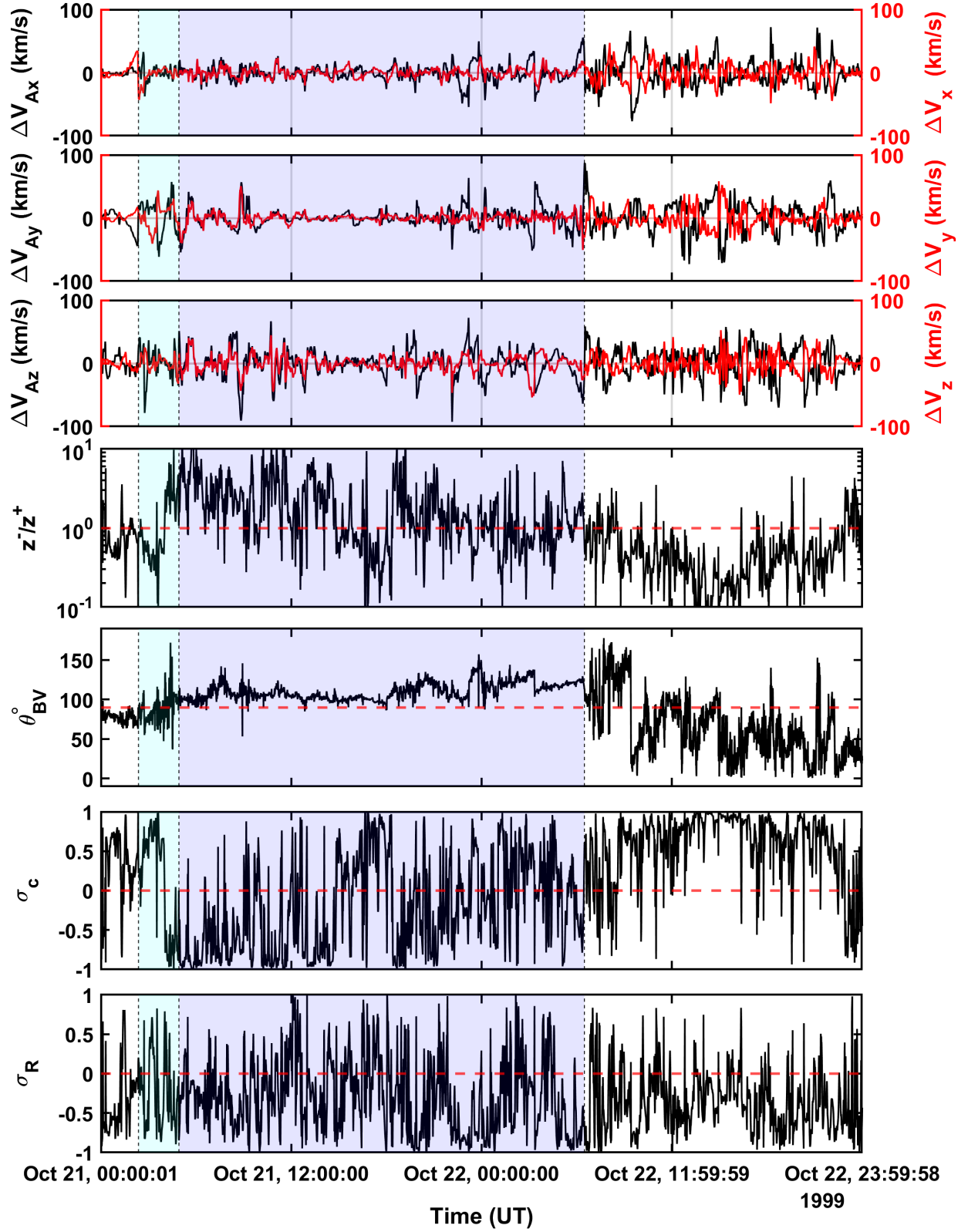


Figure 3: The top three panels compare Alfvén velocity fluctuations ΔV_{A_i} (red) to proton flow velocity fluctuations ΔV_p over time (blue). It demonstrates the Alfvénic features in MC and HSS region. Ratio of Elsässer variables z^-/z^+ shown in the fourth panel. The fifth panel depicts an angle between Alfvén velocity and solar wind speed. The bottom two panels show temporal variations of the normalised cross helicity (σ_c) and normalised residual energy (σ_R). Wind MFI and 3DP spacecraft data is used for above analysis with time cadence of 3 sec

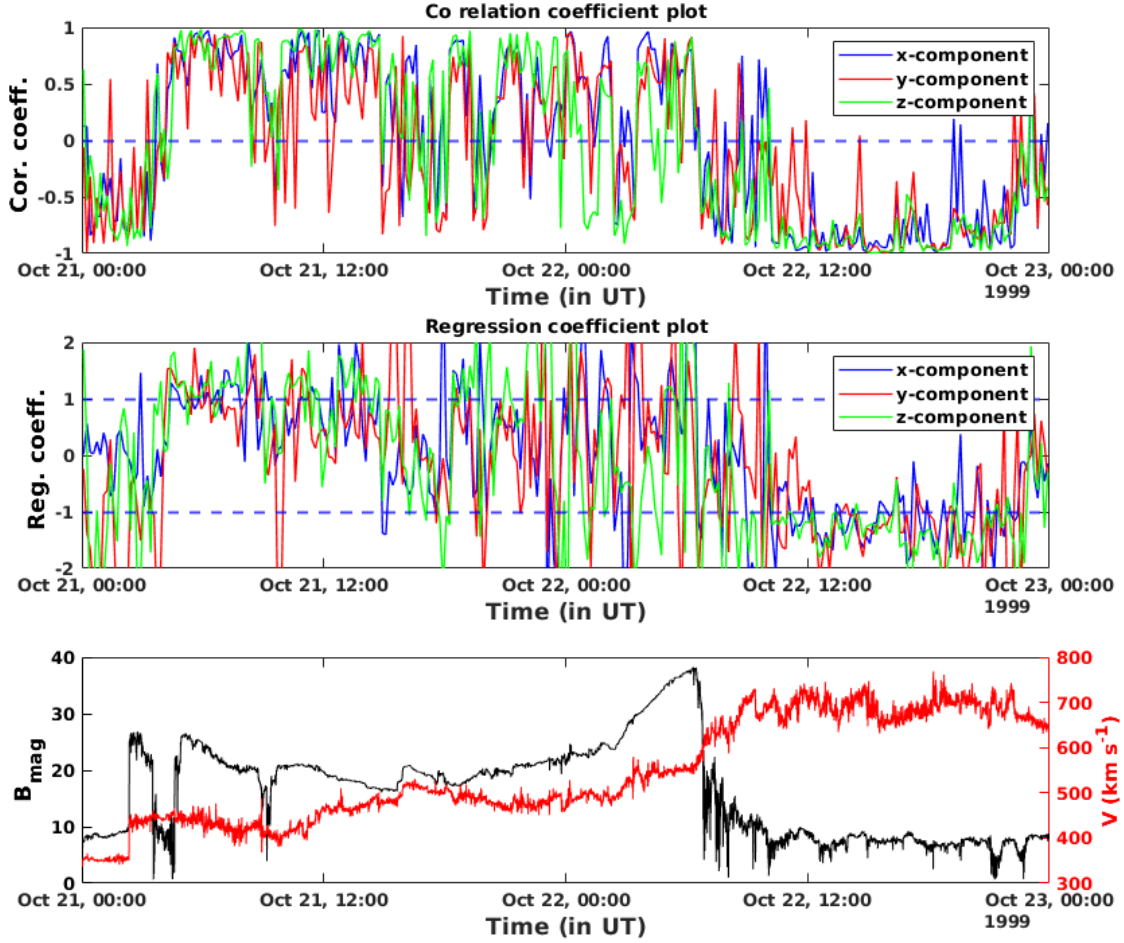


Figure 4: The top and middle panel shows the the fluctuations in correlation coefficient and the regression coefficient of each component of velocity and magnetic field with respect to time for the aforementioned scenario. The bottom panel indicates reference to the evolution of ICME and HSS using B_{mag} and solar wind speed.

Alfvénic fluctuations in the solar wind are usually a mix of two populations: outward-propagating and inward-propagating (D’Amicis & Bruno, 2015). The Walén slope (or the correlation between the magnetic field and plasma velocity) of Alfvén waves observed in the solar wind can be significantly reduced by a mix of inward and outward Alfvén waves (Yang et al., 2016; Belcher & Davis Jr, 1971; Marsch & Tu, 1993; Bruno & Carbone, 2013b). The observed Alfvén waves lies in the frequency range from 10^{-3} to 10^{-1} Hz. Therefore, to verify the temporal variations of CC and regression coefficient (RC), we passed the data of V and V_A components through the 4th order butter-worth MATLAB filter algorithm with a single broadband frequency boundaries of 10^{-3} to 10^{-1} Hz. We divided the data set under analysis into ten-minute time intervals (200 data points in each interval). Further, we estimated the CC and RC between respective components of V and V_A for each time window. Figure 4 shows the temporal variations of the CC (top panel) and RC (middle panel) for the observed Alfvénic region. The CC & RC fluctuate to ~ -1 in the HSS region corroborating strong outward flow. In contrast, both quantities fluctuate to ~ 1 in the front part of the MC, suggesting inward flow of Alfvénic fluctuations. However, we found highly fluctuating values for both the coefficients at the trailing part of MC. The Walén slope can be significantly reduced by a mix of inward and outward Alfvén waves (Yang et al., 2016; Belcher & Davis Jr, 1971; Marsch & Tu, 1993; Bruno & Carbone, 2013b). Therefore, we opine that the outward/inward Alfvén waves might have reflected from the rearer boundary of the MC. Thus, the mixing of inward and outward Alfvén waves within the trailing part of MC region is possible as suggested in the reported studies

(D'Amicis & Bruno, 2015). It is exciting to examine the inward-outward interaction region to understand parametric instabilities, and we will study that in the near future.

The generation of Alfvén wave in our study could be due to following reason; (1) steepening of a magnetosonic wave that generates the shock at the leading edge of MC (Tsurutani et al., 2011, 1988), or (2) reconnection region at the leading edge of MC (Petschek, 1964; Levy et al., 1964; Gosling et al., 2005), or (3) the velocity shear interaction between ICME and HSS (Bavassano et al., 1978; Roberts et al., 1992; Hollweg & Kaghshvili, 2011). It is important to note that Gosling et al. (2005) suggest that reconnection exhaust at the heliospheric current sheet (HCS) can generate the Alfvén waves. However, which physical process dominates at the studied regions need further detailed investigation. Moreover, (Wang et al., 2019) perform multi-spacecraft observation of MC and suggest that it can have not only unidirectional but bidirectional Alfvén waves. They also speculated that unidirectional Alfvén waves are formed within an MC by distortions in a pre-existing flux rope, while bidirectional Alfvén waves are emitted from the centre of reconnection and subsequently move outward along two foot legs of an ICME flux rope. In our study, we believe that the unidirectional Alfvén wave (inward wave) within the MC could be due to distortions of the MC. This distortion is caused by the HSS. Furthermore, this Alfvén wave embedded MC travels in the sea of HSS which has outward Alfvén wave. Thus, our study will be very important in general to understand the ICME-Solar wind interaction and associated wave origin mechanism.

Acknowledgements

The authors would like to acknowledge all individuals involved with Wind spacecraft mission development, data providing team, etc. We also acknowledge the NASA/GSFC's Space Physics Data Facilities (CDAWeb or ftp) service. We acknowledge SERB, India, since AR and OD is supported by SERB project reference file number CRG/2020/002314. also thanks to 'The Department of Science and Technology (DST)', government of India for their support (<https://dst.gov.in/>).

References

- Alfvén H., 1942, *Nature*, 150, 405
- Alves M., Echer E., Gonzalez W., 2006, *Journal of Geophysical Research: Space Physics*, 111
- Axford W., McKenzie J., 1992, in , *Solar Wind Seven*. Elsevier, pp 1–5
- Bavassano B., Bruno R., 1989a, *Journal of Geophysical Research: Space Physics*, 94, 168
- Bavassano B., Bruno R., 1989b, *Journal of Geophysical Research: Space Physics*, 94, 11977
- Bavassano B., Dobrowolny M., Moreno G., 1978, *Solar Physics*, 57, 445
- Bavassano B., Pietropaolo E., Bruno R., 2000, *Journal of Geophysical Research: Space Physics*, 105, 12697
- Belcher J., Davis Jr L., 1971, *Journal of Geophysical Research*, 76, 3534
- Belcher J., Davis Jr L., Smith E., 1969, *Journal of Geophysical Research*, 74, 2302
- Bellan P., Stasiewicz K., 1998, *Physical review letters*, 80, 3523
- Board S. S., Council N. R., et al., 2009, *Severe space weather events: Understanding societal and economic impacts: A workshop report*. National Academies Press
- Bruno R., Bavassano B., 1991, *Journal of Geophysical Research: Space Physics*, 96, 7841
- Bruno R., Carbone V., 2013a, *Living Reviews in Solar Physics*, 10, 1
- Bruno R., Carbone V., 2013b, *Living Rev. Solar Phys*, 10
- Burlaga L., Turner J., 1976, *Journal of Geophysical Research*, 81, 73
- Cally P. S., 2017, *MNRAS*, 466, 413
- Cannon P., et al., 2013, *Extreme space weather: impacts on engineered systems and infrastructure*. Royal Academy of Engineering
- Chaston C., et al., 2006, *JGR: Space Physics*, 111
- Chaston C., Carlson C., McFadden J., Ergun R., Strangeway R., 2007, *GRL*, 34
- Chen L., Zonca F., 2016, *Reviews of Modern Physics*, 88, 015008
- Cramer N. F., 2001, *The Physics of Alfvén Waves*. Wiley, doi:10.1002/3527603123

- Cross R., 1988, An introduction to Alfvén waves. A. Hilger, Bristol, England Philadelphia
- Daily W. D., 1973, *Journal of Geophysical Research*, 78, 2043
- Denton M. H., Borovsky J. E., Horne R. B., McPherson R. L., Morley S. K., Tsurutani B. T., 2008, *Eos, Transactions American Geophysical Union*, 89, 62
- Dobrowolny M., Mangeney A., Veltri P., 1980, *Physical Review Letters*, 45, 144
- D'Amicis R., Bruno R., 2015, *The Astrophysical Journal*, 805, 84
- D'Amicis R., Matteini L., Bruno R., 2019, *MNRAS*, 483, 4665
- Elsasser W. M., 1950, *Physical Review*, 79, 183
- Gamayunov K. V., Min K., Saikin A. A., Rassoul H., 2018, *Journal of Geophysical Research: Space Physics*, 123, 8533
- Gary S. P., Smith C. W., 2009, *Journal of Geophysical Research: Space Physics*, 114
- Gekelman W., 1999, *JGR: Space Physics*, 104, 14417
- Gekelman W., 2003, *JGR*, 108
- Goldstein B. E., Neugebauer M., Zhang L. D., Gary S. P., 2000, *GRL*, 27, 53
- Gosling J., Pizzo V., 1999, in , *Corotating interaction regions*. Springer, pp 21–52
- Gosling J., Pizzo V., Bame S. J., 1973, *Journal of Geophysical Research*, 78, 2001
- Gosling J., Skoug R., McComas D., Smith C., 2005, *Geophysical research letters*, 32
- Gosling J., McComas D., Roberts D., Skoug R., 2009, *The Astrophysical Journal*, 695, L213
- Gosling J., Tian H., Phan T., 2011, *The Astrophysical Journal Letters*, 737, L35
- Gupta V., et al., 2010, *Solar Physics*, 264, 165
- Hasegawa A., Chen L., 1974, *Physical Review Letters*, 32, 454
- Hasegawa A., Chen L., 1975, *Physical Review Letters*, 35, 370
- Heinemann S. G., et al., 2019, *Solar Physics*, 294, 1
- Hellinger P., Trávníček P. M., 2008, *JGR: Space Physics*, 113
- Hinton P., Bagenal F., Bonfond B., 2019, *GRL*, 46, 1242
- Hirshberg J., Alksne A., Colburn D., Bame S., Hundhausen A., 1970, *Journal of Geophysical Research*, 75, 1
- Hollweg J. V., 1975, *JGR*, 80, 908
- Hollweg J. V., Kaghshvili E. K., 2011, *The Astrophysical Journal*, 744, 114
- Hull A., Chaston C., Bonnell J., Wygant J. R., Kletzing C., Reeves G., Gerrard A., 2019, *GRL*, 46, 8597
- Hundhausen A., 1999, in , *The Many Faces of the Sun*. Springer, pp 143–200
- Jacques S., 1977, *The Astrophysical Journal*, 215, 942
- Jess D. B., Mathioudakis M., Erdélyi R., Crockett P. J., Keenan F. P., Christian D. J., 2009, *Science*, 323, 1582
- Kanekal S., et al., 2015, *Journal of Geophysical Research: Space Physics*, 120, 7629
- Keiling A., 2009, *Space Science Reviews*, 142, 73
- Keiling A., Thaller S., Wygant J., Dombeck J., 2019, *Science advances*, 5, eaav8411
- Kilpua E., Li Y., Luhmann J., Jian L., Russell C., 2012, in *Annales Geophysicae*. pp 1037–1050
- Kilpua E., Koskinen H. E., Pulkkinen T. I., 2017a, *Living Reviews in Solar Physics*, 14, 1
- Kilpua E., Balogh A., Von Steiger R., Liu Y., 2017b, *Space Science Reviews*, 212, 1271
- Krishan V., Mahajan S., 2004, *Journal of Geophysical Research: Space Physics*, 109
- Kumar A., et al., 2014, *Solar Physics*, 289, 4267
- Lepping R., et al., 1997, *Journal of Geophysical Research: Space Physics*, 102, 14049
- Levy R., Petschek H., Siscoe G., 1964, *Aiaa Journal*, 2, 2065
- Li H., Wang C., Chao J., Hsieh W., 2016, *Journal of Geophysical Research: Space Physics*, 121, 42
- Malara F., Primavera L., Veltri P., 2001, *Nonlinear Processes in Geophysics*, 8, 159
- Manchester IV W. B., Gombosi T. I., Roussev I., Ridley A., De Zeeuw D. L., Sokolov I., Powell K. G., Tóth G., 2004, *Journal of Geophysical Research: Space Physics*, 109

- Marsch E., Mangeney A., 1987, *Journal of Geophysical Research: Space Physics*, 92, 7363
- Marsch E., Tu C.-Y., 1993, *Journal of Geophysical Research: Space Physics*, 98, 21045
- Mathioudakis M., Jess D. B., Erdelyi R., 2013, *Space Science Reviews*, 175, 1
- Matteini L., Landi S., Hellinger P., Pantellini F., Maksimovic M., Velli M., Goldstein B. E., Marsch E., 2007, *GRL*, 34
- Matteini L., Hellinger P., Goldstein B. E., Landi S., Velli M., Neugebauer M., 2013, *JGR: Space Physics*, 118, 2771
- Matthaeus W. H., Goldstein M. L., 1982, *Journal of Geophysical Research: Space Physics*, 87, 10347
- Matthaeus W. H., Minnie J., Breech B., Parhi S., Bieber J., Oughton S., 2004, *Geophysical research letters*, 31
- Mavromichalaki H., Vassilaki A., 1998, *Solar Physics*, 183, 181
- McGregor S., Hudson M., Hughes W., 2014, *Journal of Geophysical Research: Space Physics*, 119, 8801
- Miyoshi Y., Kataoka R., Kasahara Y., Kumamoto A., Nagai T., Thomsen M., 2013, *Geophysical Research Letters*, 40, 4520
- Palmer I., Allum F., Singer S., 1978, *Journal of Geophysical Research: Space Physics*, 83, 75
- Perrone D., D'Amicis R., De Marco R., Matteini L., Stansby D., Bruno R., Horbury T., 2020, *Astronomy & Astrophysics*, 633, A166
- Petschek H. E., 1964, in *AAS-NASA Symposium on the Physics of Solar Flares: Proceedings of a Symposium Held at the Goddard Space Flight Center, Greenbelt, Maryland, October 28-30, 1963*. p. 425
- Raghav A. N., Kule A., 2018, *Monthly Notices of the Royal Astronomical Society: Letters*, 476, L6
- Raghav A. N., Kule A., Bhaskar A., Mishra W., Vichare G., Surve S., 2018, *The Astrophysical Journal*, 860, 26
- Raghav A. N., Choraghe K., Shaikh Z. I., 2019, *MNRAS*, 488, 910
- Riley P., Crooker N., 2004, *The Astrophysical Journal*, 600, 1035
- Riley P., Sonett C. P., Tsurutani B. T., Balogh A., Forsyth R. J., Hoogeveen G. W., 1996a, *JGR: Space Physics*, 101, 19987
- Riley P., Sonett C., Tsurutani B., Balogh A., Forsyth R., Hoogeveen G., 1996b, *Journal of Geophysical Research: Space Physics*, 101, 19987
- Roberts D., Goldstein M., Klein L., Matthaeus W., 1987, *Journal of Geophysical Research: Space Physics*, 92, 12023
- Roberts D. A., Goldstein M. L., Matthaeus W. H., Ghosh S., 1992, *JGR: Space Physics*, 97, 17115
- Rodriguez L., et al., 2016, *Solar Physics*, 291, 2145
- Salem C. S., Howes G., Sundkvist D., Bale S., Chaston C., Chen C., Mozer F., 2012, *The Astrophysical Journal Letters*, 745, L9
- Schrijver C. J., Siscoe G. L., 2010, *Heliophysics: space storms and radiation: causes and effects*. Cambridge University Press
- Shaikh D., 2010, *Monthly Notices of the Royal Astronomical Society*, 405, 2521
- Shaikh Z. I., Raghav A., Vichare G., 2019a, *MNRAS*, 490, 1638
- Shaikh Z. I., Raghav A., Vichare G., Bhaskar A., Mishra W., Choraghe K., 2019b, *MNRAS*, 490, 3440
- Shi C., Velli M., Tenerani A., Rappazzo F., Réville V., 2020, *ApJ*, 888, 68
- Singh Y., et al., 2009, *Planetary and Space Science*, 57, 318
- Stasiewicz K., et al., 2000, *Space Science Reviews*, 92, 423
- Telloni D., D'Amicis R., Bruno R., Perrone D., Sorriso-Valvo L., Raghav A. N., Choraghe K., 2021, *ApJ*, 916, 64
- Thomas T., Pfrommer C., 2019, *MNRAS*, 485, 2977
- Tomeczyk S., McIntosh S., Keil S., Judge P., Schad T., Seeley D., Edmondson J., 2007, *Science*, 317, 1192
- Tsubouchi K., 2009, *JGR: Space Physics*, 114
- Tsurutani B. T., Gonzalez W. D., 1987, *Planetary and Space Science*, 35, 405
- Tsurutani B. T., Ho C. M., 1999, *Reviews of Geophysics*, 37, 517
- Tsurutani B. T., Gonzalez W. D., Tang F., Akasofu S. I., Smith E. J., 1988, *Journal of Geophysical Research: Space Physics*, 93, 8519
- Tsurutani B. T., Ho C. M., Arballo J. K., Goldstein B. E., Balogh A., 1995, *Geophysical research letters*, 22, 3397

- Tsurutani B., Lakhina G., Verkhoglyadova O. P., Gonzalez W., Echer E., Guarnieri F., 2011, *Journal of Atmospheric and Solar-Terrestrial Physics*, 73, 5
- Tsurutani B. T., Lakhina G. S., Sen A., Hellinger P., Glassmeier K.-H., Mannucci A. J., 2018, *JGR: Space Physics*, 123, 2458
- Tu C.-Y., Marsch E., Thieme K., 1989, *Journal of Geophysical Research: Space Physics*, 94, 11739
- Vršnak B., Temmer M., Veronig A. M., 2007, *Solar Physics*, 240, 315
- Wang Y., Xue X., Shen C., Ye P., Wang S., Zhang J., 2006, *The Astrophysical Journal*, 646, 625
- Wang X., He J., Tu C., Marsch E., Zhang L., Chao J.-K., 2012, *ApJ*, 746, 147
- Wang Z., Feng X., Zheng J., 2019, *The Astrophysical Journal Letters*, 887, L18
- Webb D. F., Howard T. A., 2012, *Living Reviews in Solar Physics*, 9, 1
- Xystouris G., Sigala E., Mavromichalaki H., 2014, *Solar Physics*, 289, 995
- Yang L., Chao J., 2013, *Chin. J. Space Sci*, 33, 353
- Yang L., Lee L., Chao J., Hsieh W., Luo Q., Li J., Shi J., Wu D., 2016, *The Astrophysical Journal*, 817, 178
- Zhao X., Dyer M., 2014, *Space Weather*, 12, 448
- Zurbuchen T. H., Richardson I. G., 2006, in , *Coronal mass ejections*. Springer, pp 31–43